DOI: 10.1002/ejic.200700858

Self-Assembly of Luminescent Platinum-Salen Schiff-Base Complexes

Xingqiang Lü,[a] Wai-Yeung Wong,[a] and Wai-Kwok Wong*[a]

Keywords: Platinum / Schiff bases / Photoluminescence / Self assembly

Treatment of K_2PtCl_4 with the MeO-salen Schiff base **H_2L** [**H_2L** = *N*,*N*′-bis(3-methoxysalicylidene)ethylene-1,2-diamine] gave the precursor complex **PtL**, which, upon recrystallization from two different solvent mixtures, afforded different solvate forms of **PtL**·H_2O (**1**) and **PtL**·DMF (**2**) with different solid-state colors. The self-assembly of the **PtL** precursor with $K_2Pt(CN)_4$ or $K_2Pd(CN)_4$ leads to the isolation of isostructural compound **$[K_2(PtL)_2Pt(CN)_4]$**·1.5H_2O (**3**) or **$[K_2(PtL)_2Pd(CN)_4]$**·1.5H_2O (**4**), respectively. The solid-state structures of **1**–**4** were established by X-ray crystallography. It is interesting that the helix of the **PtL** units, along with the other two homochiral helical arrangements of K^+ and M^{2+} (M = Pt or Pd) ions, can generate a unique "fake" example of a triple-stranded helix in a 1-D helical polymeric chain. Two such triple-stranded helical chains intertwining one another can give rise to a double-stranded helix formed by intermolecular weak C–H···N hydrogen-bonding interactions with a long helical pitch of ca. 56 Å. The optical absorption and photoluminescence properties of **1**–**4** were also examined.

Introduction

The supramolecular photochemistry of square-planar platinum(II) complexes has been of intense interest in recent years, not only due to their intriguing spectroscopic and luminescent properties,[1] but also the special intermolecular interactions which could induce the stacking mode of their crystal structures[2] and the energetic order of the excited states in solid states.[3] For instance, the frequent observation of solvent-induced polymorphism of Pt^{II} complexes with bipyridine,[4] polypyridine[5] or diimine ligands[6] with extended π systems have been shown to involve π-stacking and direct Pt···Pt interactions, resulting in the formation of excimers with the characteristic red-shifted luminescence bands with respect to the luminescence from monomers. On the other hand, systems of Pt^{II} porphyrins,[7] cyclometalated Pt^{II} acetylide,[8] or Pt-salen Schiff base compounds,[9] with solid aggregation through short Pt···Pt, π-π, or C–H···π interactions, constitute an attractive class of efficient electrophosphors. However, to the best of our knowledge, research on the role of hydrogen bonding or coordination bonding between the well-defined monomers which modulates the luminescence properties of the chromophores is very sparse.[4a,10] While there is currently growing interest in the synthesis and luminescence properties of heterobimetallic 3*d*–4*f* complexes[11] and dinuclear 3*d*–4*f* Schiff-base complexes which have been employed as useful building blocks to form extended structures,[12] the use of transition-metal Schiff-base complexes as synthons for self-assembled multinuclear supramolecular systems would certainly also deserve much attention. Here, we describe new self-assembled systems consisting of platinum(II) MeO-substituted salen Schiff base **PtL** [**H_2L** = *N*,*N*′-bis(3-methoxysalicylidene)ethylene-1,2-diamine], in which the outer MeO donors of the ligands may endow hydrogen bonds or coordination bonds for self-assembling individual molecular entities. The monomeric **PtL** units are linked through a combination of intermolecular interactions to form structurally diverse metalated molecules.

[a] Department of Chemistry and Center for Advanced Luminescence Materials, Hong Kong Baptist University,
Waterloo Road, Kowloon Tong, Hong Kong, P. R. China
Fax: +852-3411-5862
E-mail: wkwong@hkbu.edu.hk

Supporting information for this article is available on the WWW under http://www.eurjic.org or from the author.

Results and Discussion

Synthesis

The ethylene-bridged MeO-salen Schiff base ligand **H_2L** was prepared according to literature method via the condensation of 1,2-diaminoethane with *o*-vanillin.[11a] Treatment of K_2PtCl_4 with **H_2L** followed by appropriate purification steps gave the precursor complex **PtL** as an orange amorphous solid (Scheme 1). Complex **PtL**·H_2O (**1**) or **PtL**·DMF (**2**) was obtained via recrystallization of **PtL** in CH_3CN/Et_2O or DMF/Et_2O, respectively. The crystal structures of **1** and **2** display the same monomer units while two different solvate forms observed account for the different solid-state colors (orange for **1** and red for **2**). The self-assembly of the **PtL** precursor with $K_2Pt(CN)_4$ or $K_2Pd(CN)_4$ leads to the isolation of isostructural polymeric compound **$[K_2(PtL)_2Pt(CN)_4]$**·1.5H_2O (**3**) or **$[K_2(PtL)_2Pd$**-

$(CN)_4]\cdot 1.5H_2O$ (**4**), respectively. Unlike complexes **1** and **2**, which are soluble in most of the common solvents, complexes **3** and **4** only have moderate solubility in DMF.

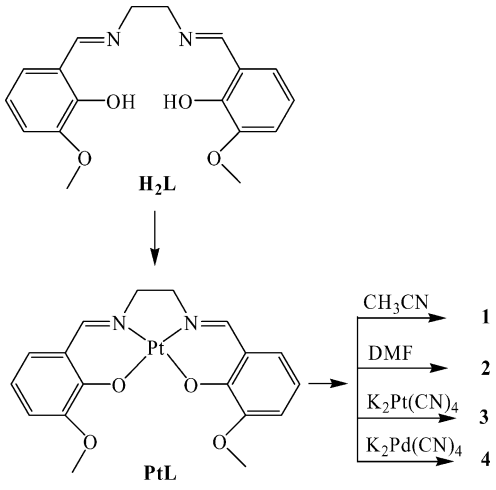

Scheme 1. Syntheses of complexes **1**–**4**.

Description of the Crystal Structures

The crystal packing diagrams of the two solvate forms **1** and **2** are depicted in Figure 1 (a) and Figure 1 (b), respectively. Table 1 lists the selected bond lengths and angles for these molecules. The structure of the individual molecule of **1** or **2** is the same with the two inner imino N and two phenolic O atoms coordinated to the platinum atom in a square-planar geometry [Pt–N, 1.951(3)–2.003(4) Å; Pt–O, 2.003(4)–2.011(3) Å] and each molecule forms a dimeric structure with its neighbor in an *anti*-parallel arrangement. For **1**, the metal dimers arise from intermolecular short π-

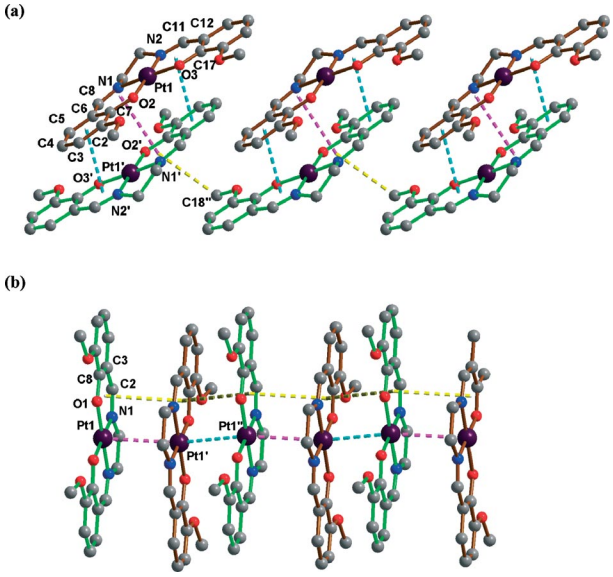

Figure 1. (a) The [**PtL**] zigzag chain in **1**, formed from intermolecular interactions [π···π interactions shown as cyan (3.728 Å, between ring Pt1–O3–C17–C12–C11–N2 and ring C2–C3–C4–C5–C6–C7) and pink (3.469 Å, between two adjacent rings Pt1–O3–C17–C12–C11–N2) striped bonds and C–H···π interactions (3.531 Å, between C18 and ring Pt1–O3–C17–C12–C11–N2) as yellow striped bonds]. Purple spheres, Pt; blue, N; red, O; ash, C. Hydrogen atoms are omitted for clarity. (b) The [**PtL**] zigzag chain in **2**, formed from intermolecular interactions [π···π interactions shown as yellow (3.495 Å, between two adjacent rings Pt1–O1–C8–C3–C2–N1) and tan (3.751 Å, between another two adjacent rings Pt1–O1–C8–C3–C2–N1) striped bonds and Pt···Pt interactions as purple (3.479 Å) and cyan (3.775 Å) striped bonds]. Purple spheres, Pt; blue, N; red, O; ash, C. Hydrogen atoms are omitted for clarity.

Table 1. Selected bond lengths [Å] and angles [°] for **1**–**4**.

Compound **1**			
Pt(1)–N(1)	1.952(3)	Pt(1)–N(2)	1.951(3)
Pt(1)–O(2)	2.011(3)	Pt(1)–O(3)	2.007(3)
N(1)–Pt(1)–N(2)	84.25(14)	O(2)–Pt(1)–O(3)	87.11(10)
N(1)–Pt(1)–O(2)	94.54(13)	N(2)–Pt(1)–O(3)	94.16(12)
Compound **2**			
Pt(1)–N(1)	1.952(5)	Pt(1)–O(1)	2.003(4)
N(1)–Pt(1)–N(1*)	84.5(3)	O(1)–Pt(1)–O(1*)	85.5(2)
N(1)–Pt(1)–O(1)	95.0(2)		
Compound **3**			
Pt(1)–N(1)	1.940(11)	Pt(1)–N(2)	1.936(9)
Pt(1)–O(2)	1.998(7)	Pt(1)–O(3)	1.972(8)
Pt(2)–N(3)	1.960(11)	Pt(2)–N(4)	1.925(11)
Pt(2)–O(6)	1.995(8)	Pt(2)–O(7)	1.984(8)
Pt(3)–C(37)	2.008(15)	Pt(3)–C(38)	1.998(14)
Pt(3)–C(39)	1.982(16)	Pt(3)–C(40)	1.984(15)
K(1)–O(1)	3.167(10)	K(1)–O(2)	2.886(10)
K(1)–O(3)	2.767(8)	K(1)–O(4)	2.929(11)
K(1)–O(7)	2.769(9)	K(1)–O(8)	2.843(9)
K(2)–O(2)	2.915(11)	K(2)–O(3)	2.927(9)
K(2)–O(5)	2.937(10)	K(2)–O(6)	2.703(9)
K(2)–O(7)	2.899(9)	K(2)–O(8)	3.351(9)
K(1)–N(7)	3.104(14)	K(1)–N(8)	2.837(13)
K(2)–N(7)	2.846(15)	K(2)–N(8)	2.717(13)
O(1)–K(1)–O(2)	48.5(2)	O(1)–K(1)–O(3)	99.4(3)
O(1)–K(1)–O(4)	124.0(3)	O(5)–K(2)–O(6)	53.8(2)
O(5)–K(2)–O(7)	105.4(3)	O(5)–K(2)–O(8)	125.3(3)
N(1)–Pt(1)–N(2)	85.1(4)	O(2)–Pt(1)–O(3)	83.6(3)
N(3)–Pt(2)–N(4)	85.3(5)	O(6)–Pt(2)–O(7)	84.2(3)
C(37)–Pt(3)–C(38)	176.3(6)	C(39)–Pt(3)–C(40)	176.6(6)
Compound **4**			
Pt(1)–N(3)	1.945(17)	Pt(1)–N(4)	1.919(19)
Pt(1)–O(6)	1.985(15)	Pt(1)–O(7)	1.990(14)
Pt(2)–N(1)	1.94(2)	Pt(2)–N(2)	1.93(2)
Pt(2)–O(2)	2.000(16)	Pt(2)–O(3)	1.995(15)
Pd(1)–C(37)	1.96(2)	Pd(1)–C(38)	2.00(3)
Pd(1)–C(39)	2.00(2)	Pd(4)–C(40)	1.99(3)
K(1)–O(3)	2.784(16)	K(1)–O(4)	2.827(17)
K(1)–O(5)	2.923(18)	K(1)–O(6)	2.772(15)
K(1)–O(7)	2.879(16)	K(1)–O(8)	3.206(17)
K(2)–O(1)	2.947(17)	K(2)–O(2)	2.723(16)
K(2)–O(3)	2.902(16)	K(2)–O(4)	3.354(17)
K(2)–O(6)	2.918(17)	K(2)–O(7)	2.941(17)
K(1)–N(5)	2.881(19)	K(1)–N(6)	3.08(2)
K(2)–N(5)	2.75(2)	K(2)–N(6)	2.83(2)
O(3)–K(1)–O(4)	54.2(5)	O(3)–K(1)–O(5)	101.0(5)
O(3)–K(1)–O(6)	80.7(5)	O(3)–K(1)–O(7)	93.1(5)
O(3)–K(1)–O(8)	124.5(5)	O(1)–K(2)–O(2)	53.6(4)
O(1)–K(2)–O(3)	105.4(5)	O(1)–K(2)–O(4)	124.0(5)
O(1)–K(2)–O(6)	74.2(5)	O(1)–K(2)–O(7)	106.8(5)
N(3)–Pt(1)–N(4)	85.0(8)	O(6)–Pt(1)–O(7)	83.9(6)
N(1)–Pt(2)–N(2)	84.3(9)	O(2)–Pt(2)–O(3)	84.9(6)
C(37)–Pd(1)–C(40)	176.2(13)	C(38)–Pd(1)–C(39)	174.0(9)

π interactions (3.469–3.728 Å), which are linked to form a zigzag arrangement (Figure 1, a) with short C–H···π hydrogen-bonding interactions (3.531 Å). Unlike **1**, where the closest Pt···Pt distance is 4.796 Å, dimorphic forms of **2** are formed via repeating short/long Pt···Pt distances (3.479 and 3.775 Å) and π-π interactions (3.495 and 3.751 Å), exhibiting an extended linear-chain skeleton (Figure 1, b). Different solvates in **1** (H_2O) and **2** (DMF) are located inside their respective multi-dimensional hydrogen-bonding networks (see Figure S4 in the electronic supporting information), and connected to their host structures by intramolecular strong O–H···O hydrogen bonding interactions (2.901–2.951 Å, ∠OHO = 132–165°) in **1** or intermolecular C–H···O hydrogen-bonding interactions (3.308 Å, ∠CHO = 139°) in **2**. This pair of structures is not described as exhibiting "pseudo-polymorphism"[13] but two different solvate forms instead,[13c] that is in contrast to the reported polymorphism in other Pt^{II} systems.[4–6]

The reaction between the **PtL** precursor and $K_2Pt(CN)_4$ or $K_2Pd(CN)_4$ leads to the isolation of isostructural complex **3** or **4**, respectively, both of which were crystallographically characterized (Table 1). In **3** and **4**, instead of short Pt···Pt, π-π, or hydrogen-bonding interactions as in **1** or **2**, only K^+ ions form coordination bonds to the monomer **PtL** [Pt–N, 1.919(19)–1.960(11) Å, Pt–O, 1.972(8)–2.000(16) Å] to afford a 1-D polymeric chain as shown in Figure 2. The K^+ ions are eight-coordinate with the usual distorted tetragonal *anti*-prism geometry, with four O atoms from one Schiff base ligand [K–O, 2.703(9)–3.354(17) Å], one inner O [K–O, 2.769(9)–2.784(16) Å] and one outer O atoms [K–O, 2.827(17)–2.843(9) Å] from the neighboring Schiff bases for K1 and two inner O atoms for K2 [K–O, 2.915(11)–2.941(17) Å], and two N atoms [K–N, 2.717(13)–3.104(14) Å] from the $M(CN)_4^{2-}$ anions (M = Pt in **3** or Pd in **4**), which induce the helical stacking of the monomeric **PtL** units. Remarkably, it is interesting that the helix of the **PtL** units, along with the other two homochiral helical arrangements of K^+ and M^{2+} (M = Pt or Pd) ions, can generate a unique "fake" example of a triple-stranded helix in a 1-D helical polymeric chain. They show two such triple-stranded helical chains intertwining one another, giving a double-stranded helix formed by intermolecular weak C–H···N hydrogen-bonding interactions (3.33–3.59 Å, ∠CHN = 134–171°) with a long helical pitch of ca. 56 Å (see supporting information, Figure S5). Solvates of H_2O in **3** and **4**, located inside their respective multi-dimensional networks, exhibit no observable interactions with the host structure.

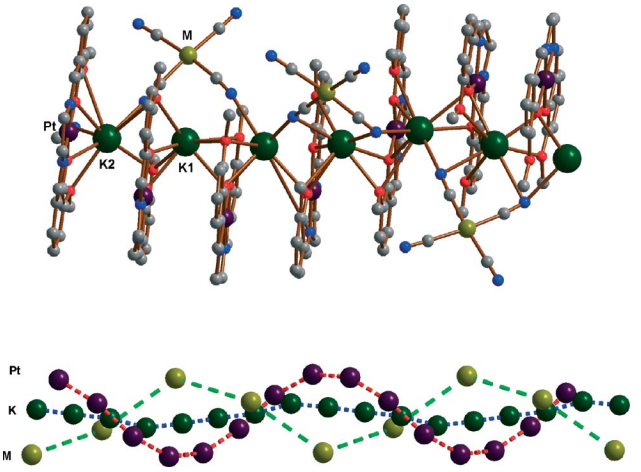

Figure 2. The 1-D helical chain (up) in **3** or **4**, with representation of metal–metal arrangements (down) as red (Pt), blue (K), or green (M, M = Pt or Pd) striped bonds. Purple spheres, Pt; blue, N; red, O; ash, C; K, aeruginous; M, bronze. Hydrogen atoms are omitted for clarity.

Absorption and Photoluminescence Properties

The photophysical data of **1**–**4** are collected in Table 2. The photoluminescence (PL) spectra of complexes **1**–**4** were recorded at 298 K in dilute DMF solutions and solid states. When dissolved in DMF, all of them gave an orange solution and exhibited analogous UV/Vis absorption

Table 2. Photophysical data of **1**–**4** at 298 K.

Complex	Medium	λ_{abs} (ε) [nm] ([10^4 dm^3 mol^{-1} cm^{-1}])	λ_{em} [nm]	τ [μs]	Φ_{em}
H_2L	DMF	331 (1.26)	498	0.006	–
1	solid	–	568, 606	–	–
	DMF	348 (1.30), 423 (0.45)	559, 605	0.12	0.10
	CH_3CN	350 (1.35), 425 (0.43)	560, 600	0.045	0.04
	CH_2Cl_2	357 (1.07), 430 (0.34), 459 sh	560, 604	0.11	0.14
	CH_3OH	347 (0.87), 420 (0.30)	557, 612	0.059	0.07
	benzene	362 (0.85), 436 (0.27), 467 sh	567, 614	0.055	0.01
2	solid	–	565, 605	–	–
	DMF	348 (1.20), 423 (0.63)	559, 607	0.11	0.29
3	solid	–	552, 610	–	–
	DMF	348 (2.06), 429 (0.64)	559, 605	0.12	0.06
4	solid	–	552, 620	–	–
	DMF	348 (1.50), 429 (0.46)	559, 604	0.11	0.10

spectra, which featured two intense absorption bands at around 340 nm [$\varepsilon = 1.30 \times 10^4$ mol^{-1} dm^3 cm^{-1}, ascribed to intraligand (IL) absorption] and 423 nm [$\varepsilon = 0.45 \times 10^4$ mol^{-1} dm^3 cm^{-1}, ascribed to metal-to-ligand charge-transfer (MLCT) absorption] (see Figure 3, a), and phosphorescent emission spectra (λ_{em} = 559 nm, with a shoulder at 604–605 nm, see Figure 3, b). Their lifetimes (τ) are similar in the microsecond regime (0.11–0.12 μs) and the quantum yields (Φ_{em}) lie within the range of 0.06–0.29. The photophysical properties of **1**–**4** in solutions are comparable to those of the reported monomeric Pt-salen complexes[9] and the excited emissive state may arise from a mixing between the ^{1}[Pt(5d) → π*(Schiff base)] MLCT state and the IL state involving the phenoxide lone pair and the π* orbital of imine. This indicates that upon dissolution, these complexes dissociated into an individual monomeric **PtL** complex and intermolecular interactions between the **PtL** units, which were observed in the solid state, did not exist in solution. Solvatochromic studies of **1** showed that both absorption bands are red-shifted in low-polarity solvents. For instance, the high-energy absorption at 347 nm in MeOH was red-shifted by ca. 1190 cm^{-1} to 362 nm in benzene, and the low-energy absorption at 420 nm by ca. 876 cm^{-1} to 436 nm with concomitant appearance of a shoulder at 467 nm in benzene (see Figures S1 and S2 in the electronic supporting information). Compared to the absorption data, the emission of **1** displays much smaller solvatochromic effects (λ_{max} at 557 nm in MeOH was red-shifted by ca. 316 cm^{-1} to 567 nm in benzene, Figure S3). Similar solvatochromic effects have also been observed for analogous Pt-salen complexes.[9]

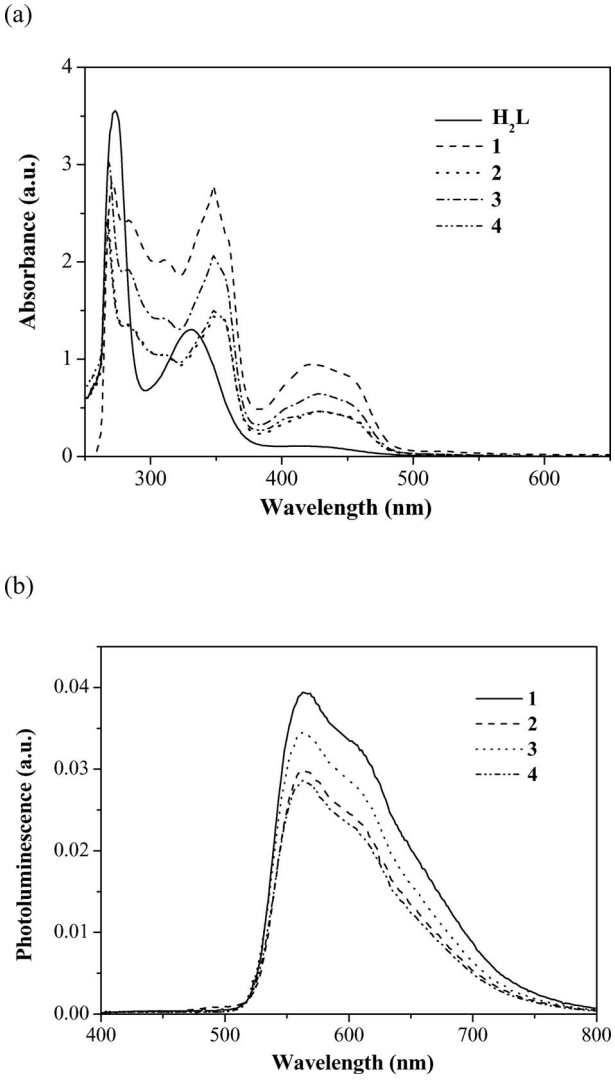

Figure 3. (a) UV/Vis and (b) PL spectra of complexes **1**–**4** in DMF solution at 2×10^{-5} M at 298 K.

At 298 K, **1**–**4** also show two intense solid-state emission peaks in the range 552–568 and 605–620 nm (as shown in Table 2 and Figure 4). It is noticeable that the significant difference in the solid-state emission spectra for **3** or **4** from that in **1** or **2** may be ascribed to the closer aggregate formation via K–O coordination in **3**–**4**, but not the hydrogen bonding and/or Pt···Pt interactions observed in **1**–**2**. Presumably, the ground-state interactions in the solid state caused by the supramolecular contacts between neighboring chromophores, viz. π-π interaction, short C–H···π hydrogen-bonding interaction, or Pt···Pt interactions (in **1** or **2**) and the coordination bonding (in **3** or **4**) may account for the observed red shifts and broadening of the emission peaks relative to those for the solution spectra,[14] and those in $[Pt(C{\equiv}CR)_4]^{2-}$ derivatives,[15] in which the combination of both Pt···Pt interactions and weak C–H···O hydrogen bonds together with the influence of solvent molecules, can result in the overall differences of the final supramolecular extended structures and their optical properties.

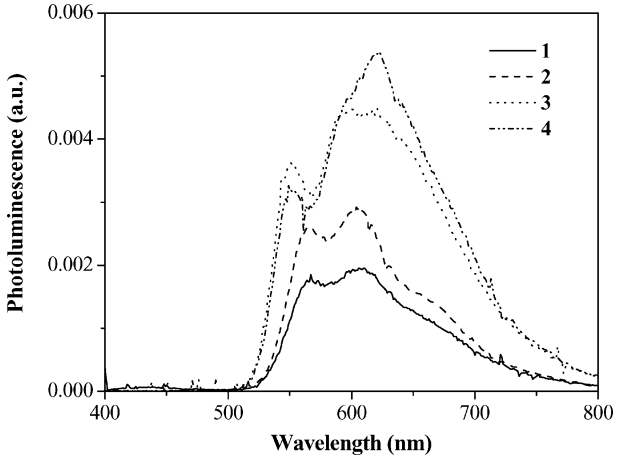

Figure 4. PL spectra of solid **1**–**4** at 298 K.

Concluding Remarks

In conclusion, we have demonstrated for the first time that hydrogen bonds from two different solvate forms and coordination bonds can induce the self-assembly of Pt^{II} MeO-salen Schiff-base complexes. These self-assembled metal complexes display interesting structural properties. It is likely that the emission properties could be fine tuned by optimization of the assay conditions from Pt^{II} emitters,

which also provides an alternative way to modify the luminescence properties of metalated light-emitting materials.

Experimental Section

General Procedures: All chemicals were commercial products of reagent grade and were used without further purification. Elemental analyses were performed with a Perkin–Elmer 240C elemental analyzer. ^{1}H NMR spectra were recorded with a JEOL EX270 spectrometer with $SiMe_4$ as an internal standard in [D_6]DMSO at room temperature. Electronic absorption spectra were recorded with a Hewlett Packard 8453 UV/Vis spectrophotometer, and steady-state visible fluorescence on a pico-N_2 laser system (PLT Time Master) with λ_{ex} = 337 nm. Quantum yields of visible emissions were computed according to literature procedures[16] using quinine sulfate in 0.1 N H_2SO_4 as the reference standard (Φ = 0.55 in air-equilibrated water).[17]

X-ray Crystallography: Geometric and intensity data were collected at 173 or 293 K using graphite-monochromated Mo-K_α radiation (λ = 0.71073 Å) with a Bruker AXS SMART 1000 CCD diffractometer. The collected frames were processed with the software SAINT[18a] and an absorption correction (SADABS)[18b] was applied to the collected reflections. The structure was solved by direct methods (SHELXTL)[19] in conjunction with standard difference Fourier techniques and subsequently refined by full-matrix least-squares analyses on F^2. Hydrogen atoms were generated in their idealized positions and all non-hydrogen atoms were assigned with anisotropic displacement parameters. Table 3 presents the crystallographic data for **1**–**4**.

CCDC-618996 (for **1**), -618997 (for **2**), -618998 (for **3**), and -618999 (for **4**) contain the supplementary crystallographic data for this paper. These data can be obtained free of charge from The Cambridge Crystallographic Data Centre via www.ccdc.cam.ac.uk/data_request/cif.

Synthesis of PtL: Sodium acetate (0.16 g, 2.0 mmol) was suspended in a solution of **H_2L** (0.33 g, 1.0 mmol) in freshly distilled DMF (10 mL). K_2PtCl_4 (0.42 g, 1.0 mmoL) in DMSO (2 mL) was added dropwise to the suspension at 80 °C. The resulting yellow solution turned orange after 5 h. After cooling, distilled water (50 mL) was added to the mixture to afford a yellow precipitate. The solid product was filtered and washed with distilled water (3 × 10 mL) to give a yellow solid, which was then dried under vacuum. The crude product was recrystallized from CH_3CN and dried to give an orange solid. Yield 280 mg (39%). ^{1}H NMR ([D_6]DMSO): δ = 8.52 (s, 2 H, HC=N), 7.05 (t, 4 H, Ph), 6.55 (t, 2 H, Ph), 3.80 (s, 4 H, CH_2), 3.75 (s, 6 H, CH_3) ppm.

Synthesis of PtL·H_2O (1): The orange solid of **PtL** (26 mg, 0.05 mmol) was added in freshly distilled CH_3CN (4 mL) and refluxed for 10 min and filtered. Diethyl ether was allowed to diffuse slowly into the clear orange solution at room temperature and orange single crystals were obtained in about 1 week. Yield 19 mg (71%). $C_{18}H_{20}N_2O_5Pt$ (539.45): calcd. C 40.08, H 3.74, N 5.19; found C 40.20, H 3.81, N 5.05. ^{1}H NMR ([D_6]DMSO): δ = 8.51 (s, 2 H, HC=N), 7.05 (t, 4 H, Ph), 6.55 (t, 2 H, Ph), 3.80 (s, 4 H, CH_2), 3.76 (s, 6 H, CH_3) ppm.

Synthesis of PtL·DMF (2): The orange solid of **PtL** (26 mg, 0.05 mmol) was added to freshly distilled DMF (3 mL) and the mixture was refluxed for 10 min and filtered. Diethyl ether was allowed to diffuse slowly into the clear orange solution at room temperature and red single crystals were obtained in about 2 weeks. Yield 19 mg (65%). $C_{21}H_{25}N_3O_5Pt$ (594.53): calcd. C 42.43, H 4.24, N 7.07; found C 42.68, H 4.37, N 7.02. ^{1}H NMR ([D_6]DMSO): δ = 8.51 (s, 2 H, HC=N), 7.94 (s, 1 H, CHO), 7.05 (t, 4 H, Ph), 6.54 (t, 2 H, Ph), 3.80 (s, 4 H, CH_2), 3.76 (s, 6 H, CH_3), 2.88 (s, 3 H, CH_3), 2.72 (s, 3 H, CH_3) ppm.

Table 3. Summary of crystal data.

	PtL·H_2O (**1**)	PtL·DMF (**2**)	[K_2(PtL)$_2$Pt(CN)$_4$]·1.5H_2O (**3**)	[K_2(PtL)$_2$Pd(CN)$_4$]·1.5H_2O (**4**)
Formula	$C_{18}H_{20}N_2O_5Pt$	$C_{21}H_{25}N_3O_5Pt$	$C_{40}H_{39}K_2N_8O_{9.5}Pt_3$	$C_{40}H_{39}K_2N_8O_{9.5}PdPt_2$
M_r	539.45	594.35	1447.26	1358.57
Crystal size [mm]	0.32 × 0.25 × 0.20	0.30 × 0.22 × 0.20	0.28 × 0.26 × 0.15	0.30 × 0.24 × 0.22
T [K]	173	293	293	173
Crystal system	monoclinic	orthorhombic	tetragonal	tetragonal
Space group	$P2_1/c$	$Pnnm$	$I4_1/cd$	$I4_1/cd$
a [Å]	9.0929(9)	19.1377(19)	24.9103(16)	24.9263(9)
b [Å]	12.8356(13)	6.9114(7)	24.9103(16)	24.9263(9)
c [Å]	14.5723(15)	15.3882(16)	28.503(3)	28.257(2)
α [°]	90	90	90	90
β [°]	93.498(2)	90	90	90
γ [°]	90	90	90	90
V [Å^3]	1697.6(3)	2034.6(4)	17502(3)	17556.9(16)
Z	4	4	16	16
$D_{calcd.}$ [g cm^{-3}]	2.111	1.941	2.197	2.056
μ [mm^{-1}]	8.290	6.936	9.823	7.018
F(000)	1028	1160	10928	10416
2θ range [°]	54.12	54.08	54.06	54.08
No. of reflections collected	9384	9895	42139	38577
No. of unique reflections	3704	2309	7817	9518
R_{int}	0.0269	0.0286	0.0705	0.0781
No. of observed reflections with $I > 2.0\sigma(I)$	3002	1932	6500	6850
No. of parameters	243	159	564	570
R_1 [$I > 2.0\sigma(I)$][a]	0.0227	0.0244	0.0396	0.0760
wR_2 (all data)[a]	0.0511	0.0724	0.1063	0.2178
GoF on F^2[b]	1.027	1.006	1.104	1.027

[a] $R_1 = \Sigma \, ||F_o| - |F_c|| / \Sigma \, |F_o|$. $wR_2 = \{\Sigma \, [w(F_o^2 - F_c^2)^2] / \Sigma \, [w(F_o^2)^2]\}^{1/2}$. [b] GoF = $[(\Sigma w|F_o| - |F_c|)^2 / (N_{obs} - N_{param})]^{1/2}$.

Synthesis of $[K_2(PtL)_2Pt(CN)_4]\cdot 1.5H_2O$ (3): The white solid of $K_2Pt(CN)_4$ (5.0 mg, 0.03 mmol) was added to a solution of **PtL** (15 mg, 0.06 mmol) in DMF (4 mL) and the resultant solution was stirred for 30 min and filtered. Diethyl ether was allowed to diffuse slowly into the clear orange solution at room temperature and red single crystals were obtained in 3 weeks. Yield 32 mg (73%). $C_{40}H_{39}K_2N_8O_{9.5}Pt_3$ (1447.24): calcd. C 33.20, H 2.72, N 7.74; found C 33.28, H 3.07, N 7.62. ^{1}H NMR (δ_H, [D$_6$]DMSO): δ = 8.51 (s, 2 H, HC=N), 7.06 (t, 4 H, Ph), 6.56 (t, 2 H, Ph), 3.81 (s, 4 H, CH_2), 3.77 (s, 6 H, CH_3) ppm.

Synthesis of $[K_2(PtL)_2Pd(CN)_4]\cdot 1.5H_2O$ (4): The complex was prepared in the same way as **3** except that $K_2Pd(CN)_4$ was used instead of $K_2Pt(CN)_4$ and a red solid was obtained in 67% yield (30 mg). $C_{40}H_{39}K_2N_8O_{9.5}PdPt_2$ (1358.58): calcd. C 35.56, H 2.89, N 8.25; found C 35.38, H 3.27, N 8.12. ^{1}H NMR ([D$_6$]DMSO): δ = 8.57 (s, 2 H, HC=N), 7.10 (t, 4 H, Ph), 6.60 (t, 2 H, Ph), 3.85 (s, 4 H, CH_2), 3.77 (s, 6 H, CH_3) ppm.

Supporting Information (see also the footnote on the first page of this article): Absorption and emission spectra of **1** in various solvents, and different views of the crystal stackings of **1** and **2**.

Acknowledgments

This work was supported by a CERG grant from the Research Grants Council of the Hong Kong SAR, P. R. China (project no. HKBU 2038/02P) and Hong Kong Baptist University.

[1] a) V. H. Houlding, V. M. Miskowski, *Coord. Chem. Rev.* **1991**, *111*, 145–152; b) D. R. McMillin, J. J. Moore, *Coord. Chem. Rev.* **2002**, *229*, 113–121; c) W. L. Fleman, W. B. Connick, *Comment, Inorg. Chem.* **2002**, *23*, 205–230.

[2] a) C. N. Pettijohn, E. B. Jochnowitz, B. Chuong, J. K. Nagle, A. Vogler, *Coord. Chem. Rev.* **1998**, *171*, 85–92; b) M. Hissler, J. E. McGarrah, W. B. Connick, D. K. Geiger, S. D. Cummings, R. Eisenberg, *Coord. Chem. Rev.* **2000**, *208*, 115–137; c) P. Batail, *Chem. Rev.* **2004**, *104*, 4887–4890.

[3] a) M. R. Bryce, *J. Mater. Chem.* **2000**, *10*, 589–598; b) K. E. Dungey, B. D. Thompson, N. A. P. Kane-Maguire, L. L. Wright, *Inorg. Chem.* **2000**, *39*, 5192–5196; c) J. L. Segura, N. Martin, *Angew. Chem. Int. Ed.* **2001**, *40*, 1372–1409; d) S.-C. Chan, M. C. W. Chan, Y. Wang, C.-M. Che, K.-K. Cheung, N. Zhu, *Chem. Eur. J.* **2001**, *7*, 4180–4190; e) Y.-Y. Lin, S.-C. Chan, M. C. W. Chan, Y.-J. Hou, N. Zhu, C.-M. Che, Y. Liu, Y. Wang, *Chem. Eur. J.* **2003**, *9*, 1263–1272; f) J. O. Segura, J. Becher, *Eur. J. Org. Chem.* **2003**, 3245–3266; g) T. Otsubo, K. Takimiya, *Bull. Chem. Soc. Jpn.* **2004**, *77*, 43–58.

[4] a) V. M. Miskowski, V. H. Houlding, *Inorg. Chem.* **1993**, *32*, 2518–2524; b) W. B. Connick, L. M. Henling, R. E. Marsh, H. B. Gray, *Inorg. Chem.* **1996**, *35*, 6261–6265.

[5] a) J. S. Field, R. J. Haines, D. R. McMillin, G. C. Summerton, *J. Chem. Soc. Dalton Trans.* **2002**, 1369–1376; b) V. W.-W. Yam, K. M.-C. Wong, N. Zhu, *J. Am. Chem. Soc.* **2002**, *124*, 6506–6507.

[6] a) V. M. Miskowski, V. H. Houlding, *Inorg. Chem.* **1989**, *28*, 1529–1533; b) V. M. Miskowski, V. H. Houlding, *Inorg. Chem.* **1991**, *30*, 4446–4452; c) S. Delahaya, C. Loosli, S.-X. Liu, S. Decurtins, G. Labat, A. Neels, A. Loosli, T. R. Ward, A. Hauser, *Adv. Funct. Mater.* **2006**, *16*, 286–295.

[7] a) M. A. Baldo, D. F. O'Brien, Y. You, A. Shoustikov, S. Sibley, M. E. Thompson, S. R. Forrest, *Nature* **1998**, *395*, 151–154; b) R. C. Kwong, S. Sibley, T. Dubovoy, M. A. Baldo, S. R. Forrest, M. E. Thompson, *Chem. Mater.* **1999**, *11*, 3709–3713; c) C. Adachi, M. A. Baldo, S. R. Forrest, M. E. Thompson, *Appl. Phys. Lett.* **2000**, *77*, 904–906; d) C. Adachi, M. A. Baldo, M. E. Thompson, S. R. Forrest, *J. Appl. Phys.* **2001**, *90*, 5048–5051.

[8] a) W. Lu, B. X. Mi, M. C. W. Chan, Z. Hui, N. Zhu, S. T. Lee, C.-M. Che, *Chem. Commun.* **2002**, 206–207; b) W. Lu, B. X. Mi, M. C. W. Chan, Z. Hui, C.-M. Che, N. Zhu, S. T. Lee, *J. Am. Chem. Soc.* **2004**, *126*, 4958–4971.

[9] a) C.-M. Che, S.-C. Chan, H.-F. Xiang, M. C. W. Chan, Y. Liu, Y. Wang, *Chem. Commun.* **2004**, 1484–1485; b) H.-F. Xiang, S.-C. Chan, K. K.-Y. Wu, C.-M. Che, P. T. Lai, *Chem. Commun.* **2005**, 1408–1410.

[10] T. J. Wadas, R. J. Lachicotte, R. Eisenberg, *Inorg. Chem.* **2003**, *42*, 3772–3778.

[11] a) W.-K. Lo, W.-K. Wong, J. Guo, W.-Y. Wong, K.-F. Li, K.-W. Cheah, *Inorg. Chim. Acta* **2004**, *357*, 4510–4521; b) W.-K. Wong, H.-Z. Liang, W.-Y. Wong, Z.-W. Cai, K.-F. Li, K.-W. Cheah, *New J. Chem.* **2002**, *26*, 275–278; c) X.-P. Yang, R. A. Jones, V. Lynch, M. M. Oye, A. L. Holmes, *Dalton Trans.* **2005**, 849–851; d) X.-P. Yang, R. A. Jones, *J. Am. Chem. Soc.* **2005**, *127*, 7686–7687.

[12] R. Gheorghe, M. Andruh, A. Muller, M. Schmidtmann, *Inorg. Chem.* **2002**, *41*, 5314–5316.

[13] a) W. C. McCrone in *Physics and Chemistry of the Organic Solid State* (Eds.: D. Fox, M. M. Labes, A. Weissberger), Wiley-Interscience, New York, **1965**, vol. 2; b) J. A. R. P. Sarma, G. R. Desiraju in *Crystal Engineering: The Design and Application of Functional Solids* (Eds.: K. R. Seddon, M. J. Zaworotko), Kluwer, Dordrecht, **1999**, vol. 539, pp. 325–356; c) K. R. Seddon, *Cryst. Growth Des.* **2004**, *4*, 1087–1088; d) G. R. Desiraju, *Cryst. Growth Des.* **2004**, *4*, 1089–1090.

[14] a) P. Coppens, S.-L. Zheng, M. Gembicky, M. Messerschmidt, M. Dominiak, *CrystEngComm* **2006**, *8*, 735–741; b) M. A. Omary, M. A. Rawashdeh, M. W. Alexander, O. Elbjeirami, T. Grimes, T. R. Cundari, *Inorg. Chem.* **2005**, *44*, 8200–8210; c) H. V. Rasika Dias, H. V. K. Diyabalanage, M. G. Eldabaja, O. Elbjeirami, M. A. Rawashdeh-Omary, M. A. Omary, *J. Am. Chem. Soc.* **2005**, *127*, 7489–7501.

[15] B. Gil, J. Forniés, J. Gómez, E. Lalinde, A. Martín, M. T. Moreno, *Inorg. Chem.* **2006**, *45*, 7788–7798.

[16] C. A. Parker, W. T. Rees, *Analyst* **1960**, *85*, 587–600.

[17] S. R. Meech, D. C. Phillips, *J. Photochem.* **1983**, *23*, 193–217.

[18] a) *SAINT*+, ver. 6.02a, Bruker Analytical X-ray Systems, Inc., Madison, WI, **1998**; b) G. M. Sheldrick, *SADABS*, Empirical Absorption Correction Program, University of Göttingen, Germany, **1997**.

[19] G. M. Sheldrick, *SHELXTL*, ver. 5.1, Madison, WI, **1997**.

Received: August 16, 2007
Published Online: December 6, 2007

